The Sunyaev-Zeldovich Effect

- microwave background photons can be Compton scattered by hot electrons in the gas in galaxy clusters:

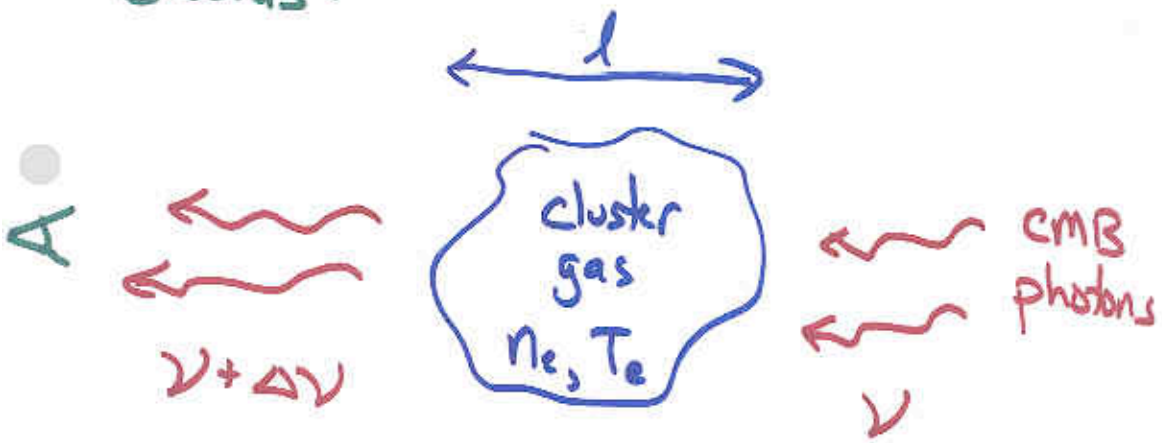

$$\left(\frac{\Delta T}{T}\right)_{CMB} = -2\frac{\sigma_T k}{m_e c^2}\int n_e T_e \, dl$$

Cluster Data

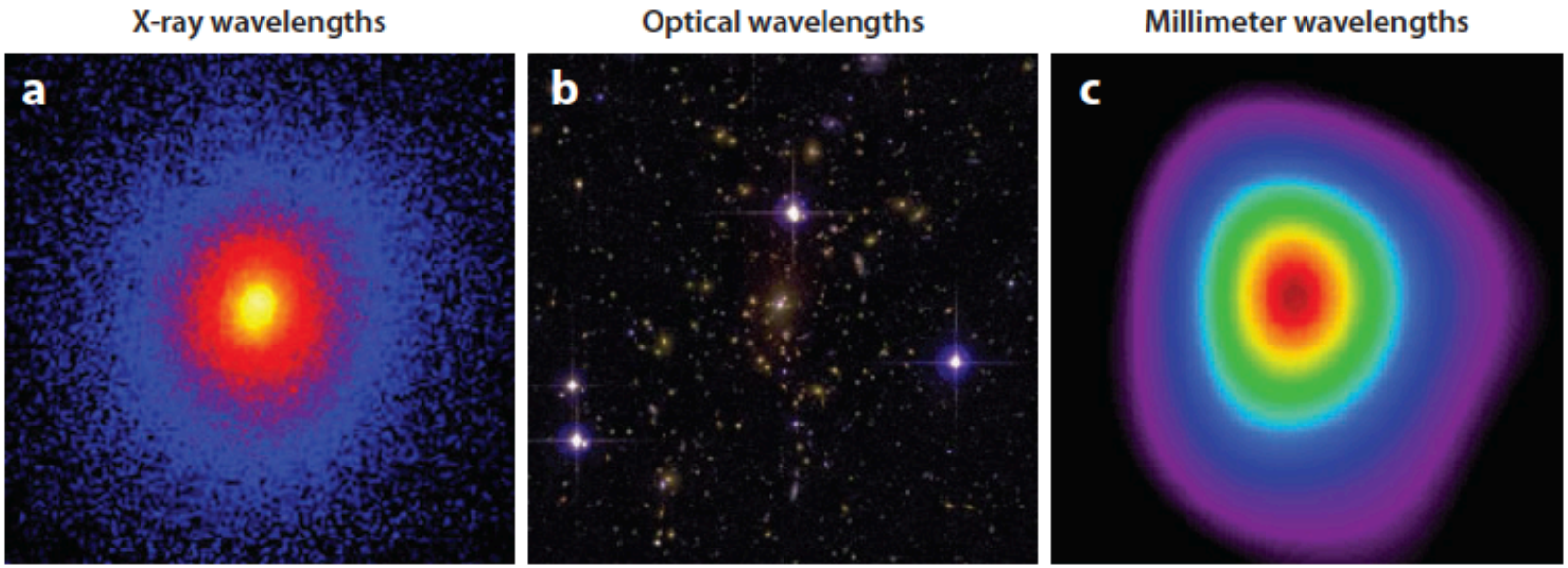

Figure 7

Images of Abell 1835 ($z = 0.25$) at (*a*) X-ray, (*b*) optical, and (*c*) millimeter wavelengths, exemplifying the regular multiwavelength morphology of a massive, dynamically relaxed cluster. All three images are centered on the X-ray peak position and have the same spatial scale, 5.2 arcmin or ~1.2 Mpc on a side (extending out to $\sim r_{2,500}$; Mantz et al. 2010a). Figure credits: (*a*) X-ray: *Chandra X-ray Observatory*/A. Mantz; (*b*) optical: Canada-France-Hawaii Telescope/A. von der Linden et al.; (*c*) millimeter: Sunyaev Zel'dovich Array/D. Marrone.

Allen+ ARAA 2011

Sunyaev-Zeldovich effect on CMB spectrum

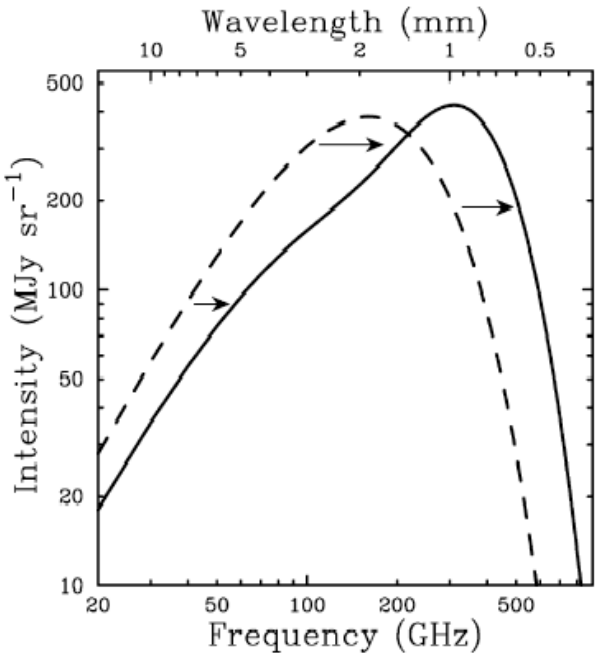

Figure 1 The cosmic microwave background (CMB) spectrum, undistorted (*dashed line*) and distorted by the Sunyaev-Zel'dovich effect (SZE) (*solid line*). Following Sunyaev & Zel'dovich (1980a) to illustrate the effect, the SZE distortion shown is for a fictional cluster 1000 times more massive than a typical massive galaxy cluster. The SZE causes a decrease in the CMB intensity at frequencies $\lesssim$218 GHz and an increase at higher frequencies.

Observed in Abell 2163

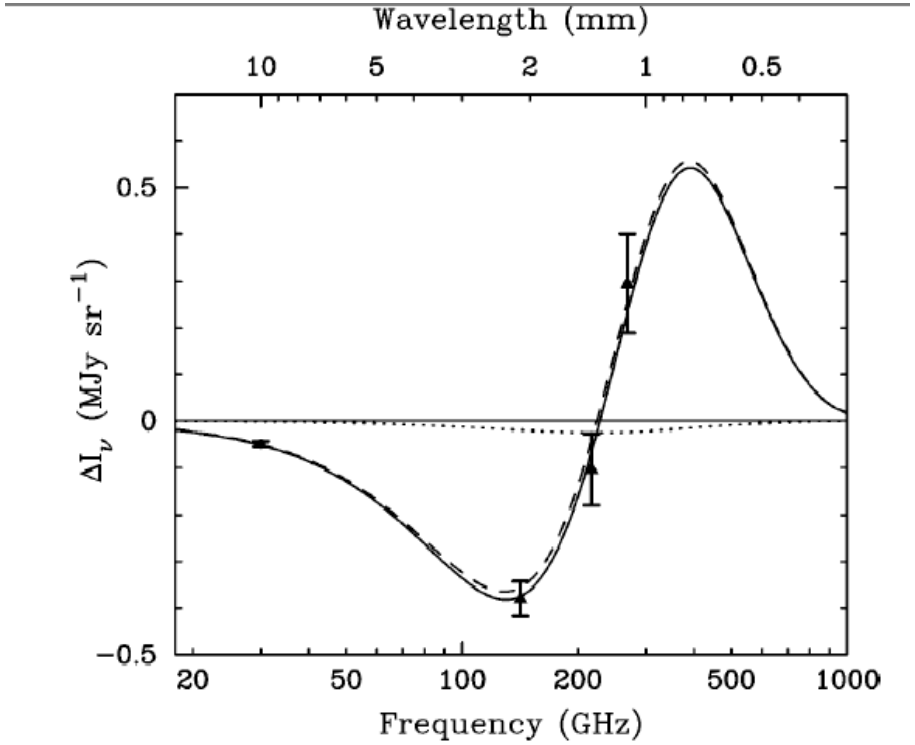

Figure 4 The measured SZE spectrum of Abell 2163. The data point at 30 GHz is from the Berkeley-Illinois-Maryland-Association (BIMA) array (LaRoque et al. 2002), at 140 GHz it is the weighted average of Diabolo and SuZIE measurements (Desert et al. 1998, Holzapfel et al. 1997) (*filled square*), and at 218 GHz and 270 GHz from SuZIE (Holzapfel et al. 1997) (*filled triangles*). The best fit thermal and kinetic SZE spectra are shown by the dashed and dotted lines, respectively, with the spectra of the combined effect shown by the solid line. The limits on the Compton y-parameter and the peculiar velocity are $y_0 = 3.56^{+0.41+0.27}_{-0.41-0.19} \times 10^{-4}$ and $v_p = 410^{+1030+460}_{-850\ -440}$ km s^{-1}, respectively, with statistical followed by systematic uncertainties at 68% confidence (Holzapfel et al. 1997, LaRoque et al. 2002).

Carlstrom+ ARAA 2002

SZ effect shows up on much smaller angular scales than CMB

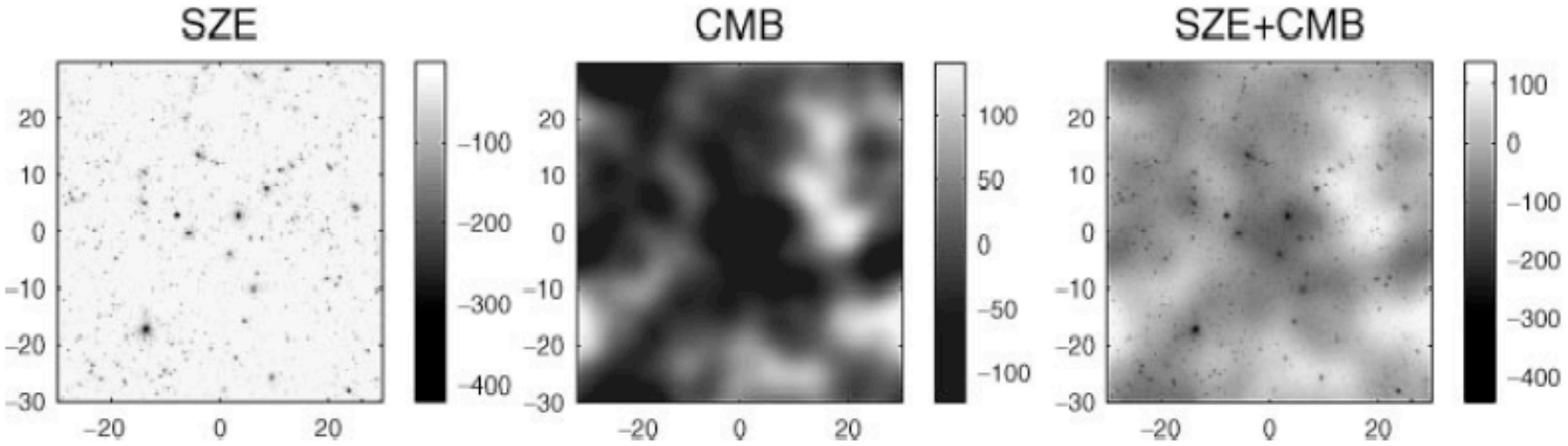

Figure 3 Illustration of the characteristic angular scales of primary CMB anisotropy and of the SZE. The images each cover one square degree and the gray scales are in μK. (*Left*) An image of the SZE from many galaxy clusters at 150 GHz (2 mm) from a state-of-the-art hydrodynamic simulation (Springel et al. 2001). The clusters appear point-like at this angular scale. (*Center*) A realization of CMB anisotropy for a ΛCDM cosmology. (*Right*) The combination of the CMB and SZE signals. Note, the SZE can be distinguished readily from primary CMB anisotropy, provided the observations have sufficient angular resolution.

Carlstrom+ ARAA 2002

SZ detections of clusters

Note: SZ signal is independent of distance!

$$\left(\frac{\Delta T}{T}\right)_{CMB} = -2\frac{g_k}{m_e c^2}\int n_e T_e \, dl$$

(But getting *other* information about the clusters becomes hard at high redshift.)

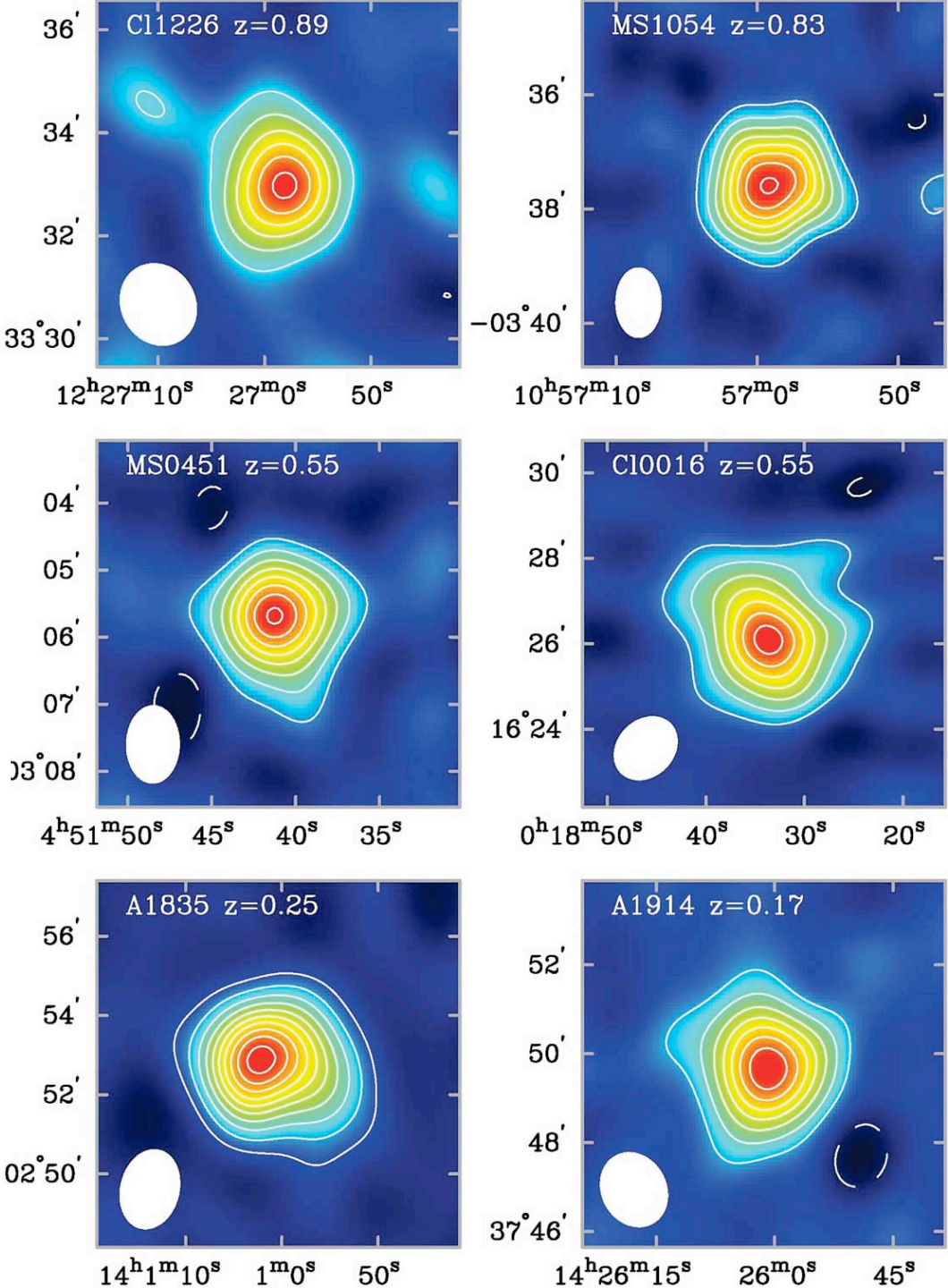

Distance Determination:

#1: determine $\Delta T/T$ from millimeter wave observation

$$\underset{\text{CMB}}{\Delta T} \sim \int \underbrace{dl}_{=D_A\theta} \overbrace{n_e T_e}^{e^-}$$

(assuming sphericity)

#2: determine X-ray surface brightness

$$S_x \sim \int \underbrace{dl}_{D_A\theta} \overbrace{n_e^2 \Lambda_e}^{e^-}$$

(Λ_e: cooling function, not cosmo. const.)

#3: solve for D_A

$$D_A \sim \frac{\Delta T^2 \Lambda_e}{S_x T_e^2 \theta}$$

for low-z, $V = H_0 D_A \rightarrow$ get H_0

for all-z $D_A = f(\text{cosmology}) \rightarrow$ get cosmology

Built in assumptions / issues:

→ we observe surface density & projected temperature, but we need 3-d quantities

↳ modeling

→ assume sphericity
isothermality
hydrostatic equilibrium
} is this OK?

→ assume smoothness, i.e. that

$$C \equiv \frac{\langle n_e^2 \rangle^{1/2}}{\langle n_e \rangle} \approx 1$$

↑ clumpiness

$(H_0 \sim C^2)$

i.e. clumpiness leads to overestimated H_0

Cluster
X-ray Images

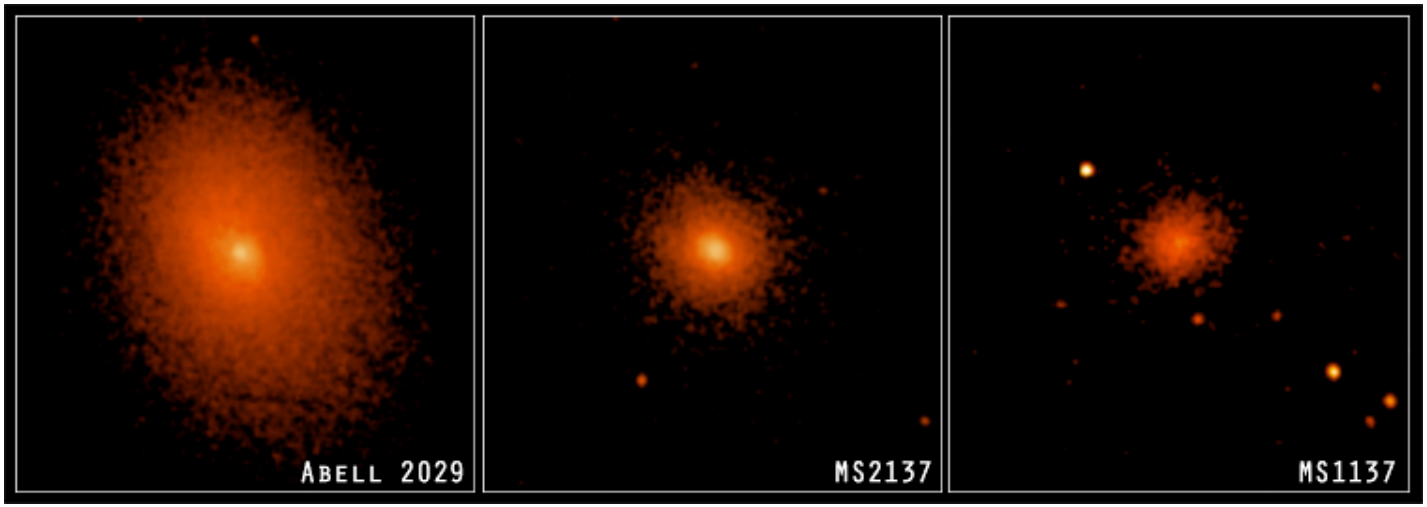

Abell 2125

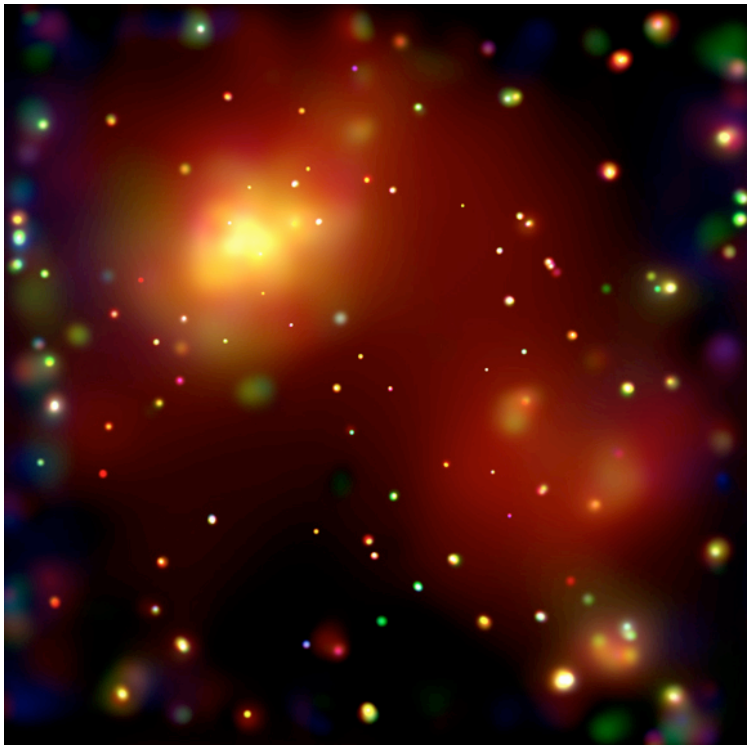

Coma

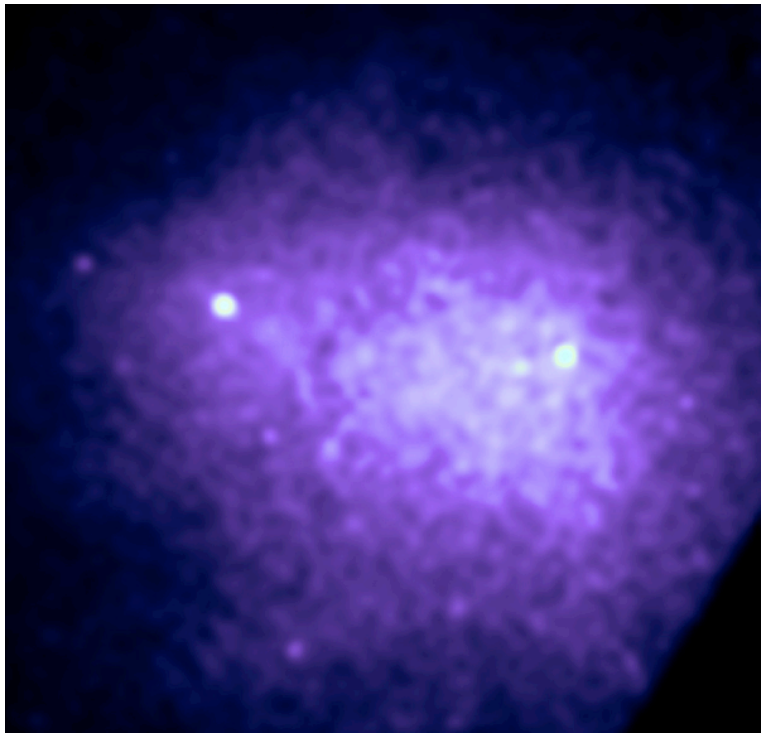

Early SZ H0 Results…. all over the map.

Table 2 The Hubble constant from S-Z and X-ray measurements

Cluster	kT_e (KeV)	β_n	θ_c	H_0 (km s^{-1} Mpc^{-1})	Reference
A478	6.56 ± 0.09	0.67 ± 0.03	$1.93' \pm 0.30'$	32^{+19}_{-15}	Myers et al (1995)
A665	8.18 ± 0.53	0.66	$1.6'$	40 ± 9	Birkinshaw et al (1991)
A1656	9.10 ± 0.40	0.75 ± 0.03	$10.5' \pm 0.60'$	74^{+29}_{-24}	Herbig et al (1994)
A2142	8.68 ± 0.12	1	$3.69' \pm 0.14'$	57^{+61}_{-39}	Myers et al (1995)
A2163	14.6 ± 0.55	0.62 ± 0.01	$1.20' \pm 0.05'$	82^{+35}_{-22}	Holzapfel et al (1995)
A2218	6.70 ± 0.45	0.65	$1'$	24 ± 11	McHardy et al (1990)
A2218	6.70 ± 0.45	0.65	$1'$	65 ± 25	Birkinshaw & Hughes (1994)
A2218	6.70 ± 0.45	0.64	$1'$	38^{+18}_{-16}	Jones (1994)
A2256	7.51 ± 0.11	0.795 ± 0.020	$5.33' \pm 0.20'$	76^{+22}_{-19}	Myers et al (1995)

Table 4. Angular size distances and corresponding values of H_0 for two cosmologies for the five clusters in the sample. Errors quoted are just random – there is an additional 14 per cent systematic error on all the clusters. Also given are the central temperature decrements using the best normalization of the fitted β-model to the SZ data.

Cluster	Redshift	D_A (Mpc)	H_0 (SCDM)	H_0 (ΛCDM)	ΔT_0 (μK)
A697	0.282	1050^{+380}_{-280}	52^{+18}_{-14}	59^{+21}_{-16}	-1047 ± 160
A773	0.217	600^{+220}_{-160}	77^{+28}_{-21}	85^{+31}_{-23}	-737 ± 85
A1413	0.143	590^{+280}_{-190}	57^{+27}_{-17}	61^{+29}_{-18}	-863 ± 242
A1914	0.217	390^{+180}_{-125}	119^{+56}_{-35}	129^{+60}_{-38}	-864 ± 305
A2218	0.171	1250^{+525}_{-370}	31^{+13}_{-9}	34^{+15}_{-10}	-797 ± 205

(Jones+05)

Abell 1914 (Feldmeier+04)

Early SZ H0 Results…. all over the map.

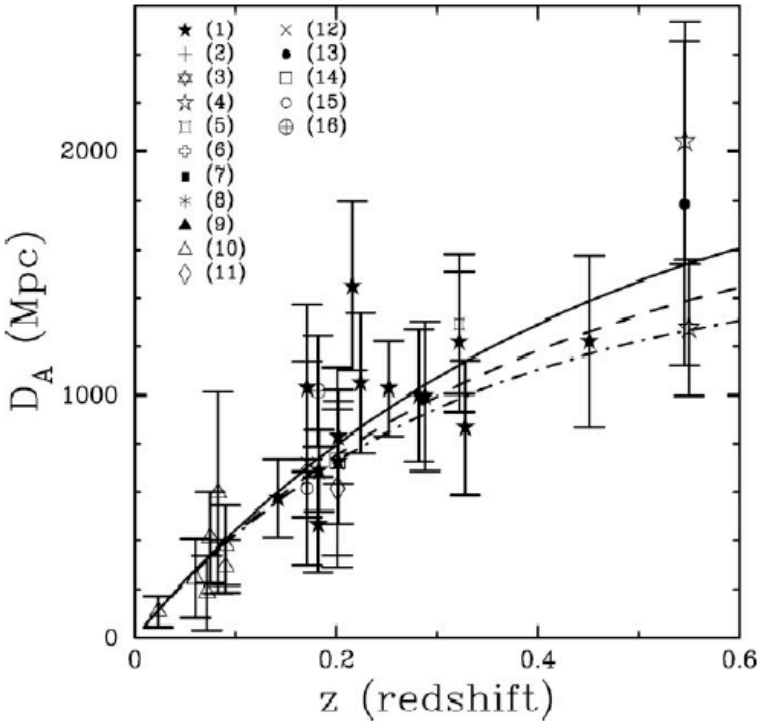

Figure 9 SZE-determined distances versus redshift. The theoretical angular diameter distance relation is plotted for three different cosmologies, assuming $H_0 = 60$ km s^{-1} Mpc^{-1}. $\Omega_M = 0.3$, $\Omega_\Lambda = 0.7$ (*solid line*), $\Omega_M = 0.3$, $\Omega_\Lambda = 0$ (*dashed line*), and $\Omega_M = 1.0$, $\Omega_\Lambda = 0$ (*dot-dashed line*). The clusters are beginning to trace out the angular diameter distance relation. References: (1) Reese et al. 2002; (2) Pointecouteau et al. 2001; (3) Mauskopf et al. 2000a; (4) Reese et al. 2000; (5) Patel et al. 2000; (6) Grainge et al. 2000; (7) Saunders et al. 2000; (8) Andreani et al. 1999; (9) Komatsu et al. 1999; (10) Mason et al. 2001, Mason 1999, Myers et al. 1997; (11) Lamarre et al. 1998; (12) Tsuboi et al. 1998; (13) Hughes & Birkinshaw 1998; (14) Holzapfel et al. 1997; (15) Birkinshaw & Hughes 1994; (16) Birkinshaw et al. 1991.

Carlstrom+ ARAA 2002

Better data, more clusters

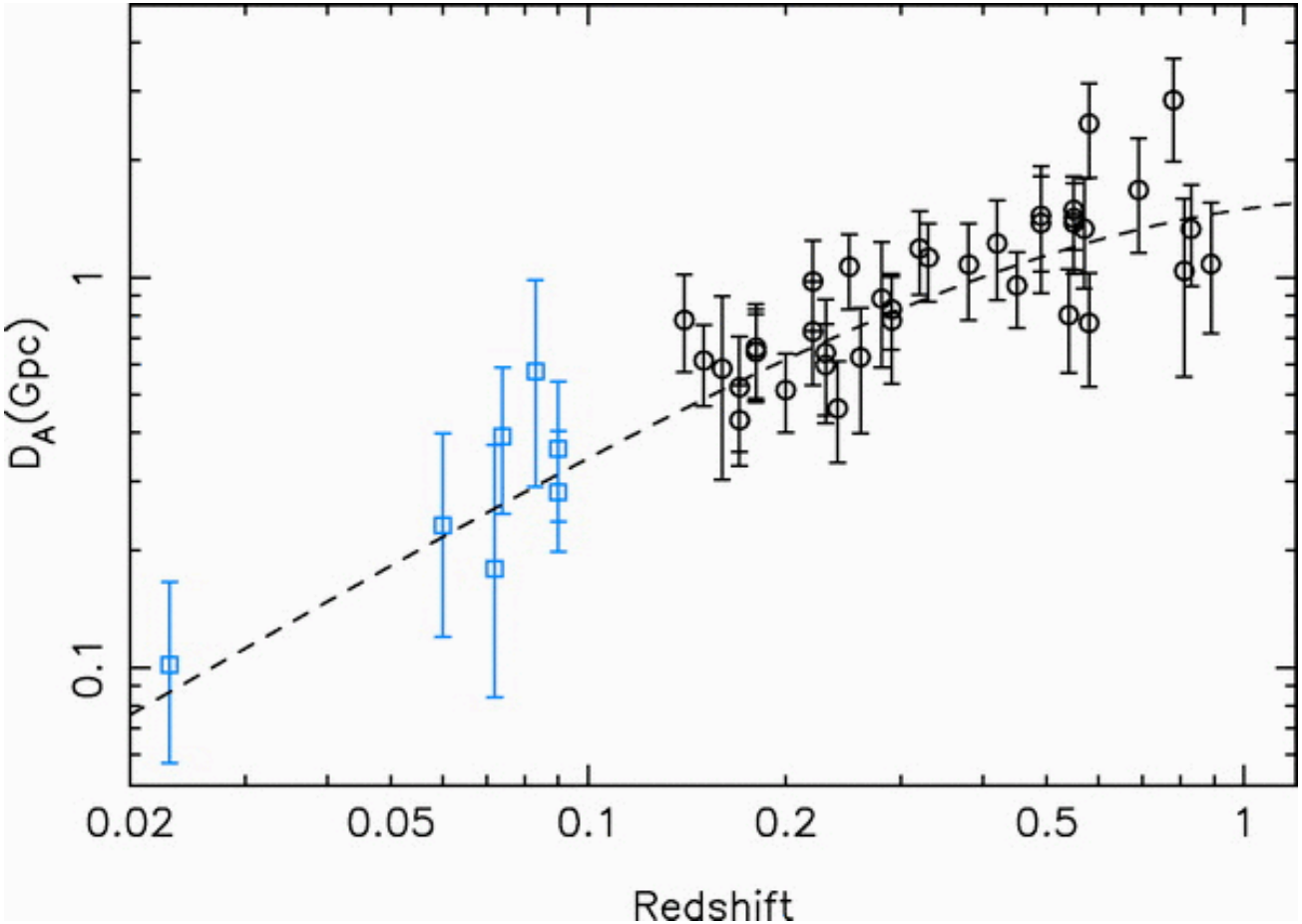

H_0=77 ± 4 ± 9 km/s/Mpc for Ω_M=0.3, Ω_Λ=0.7

Bonamente+ 2006

Gravitational Lensing

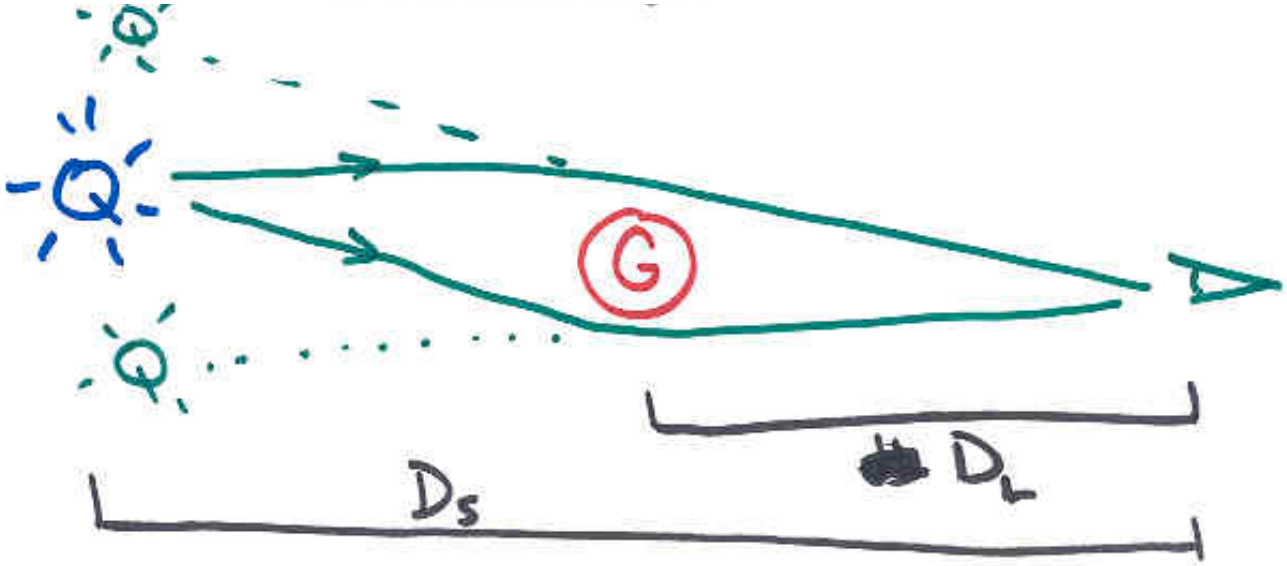

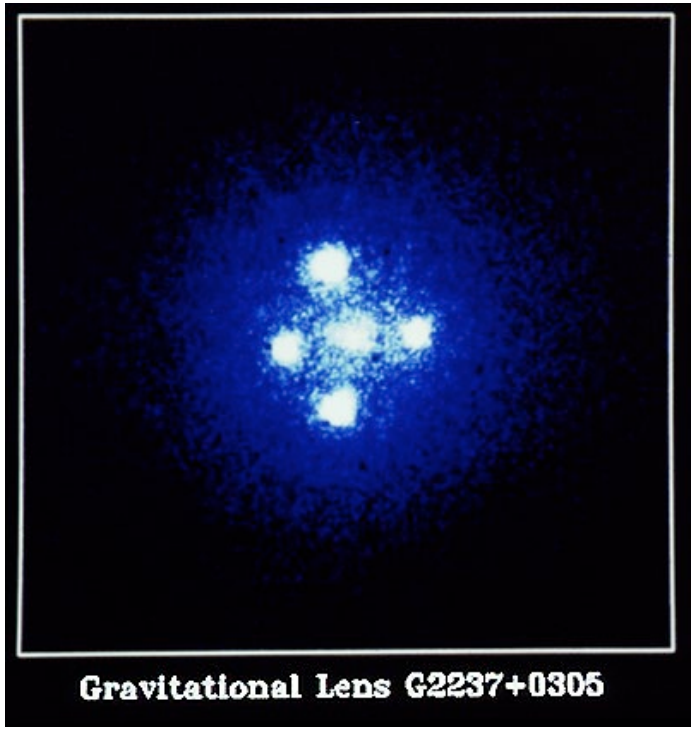

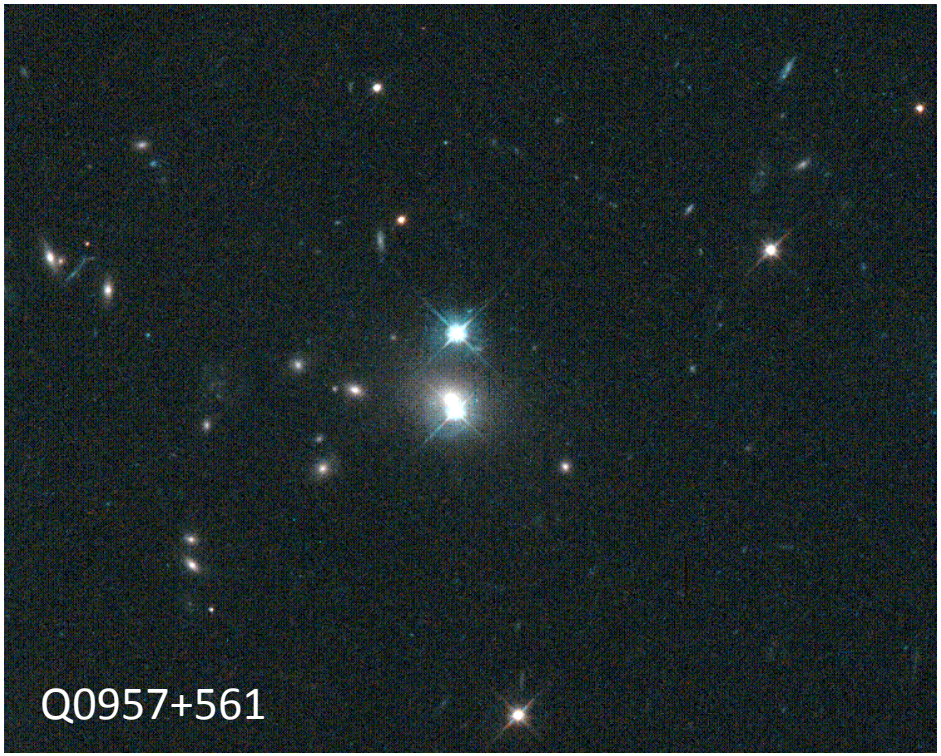

Variability Time Delays

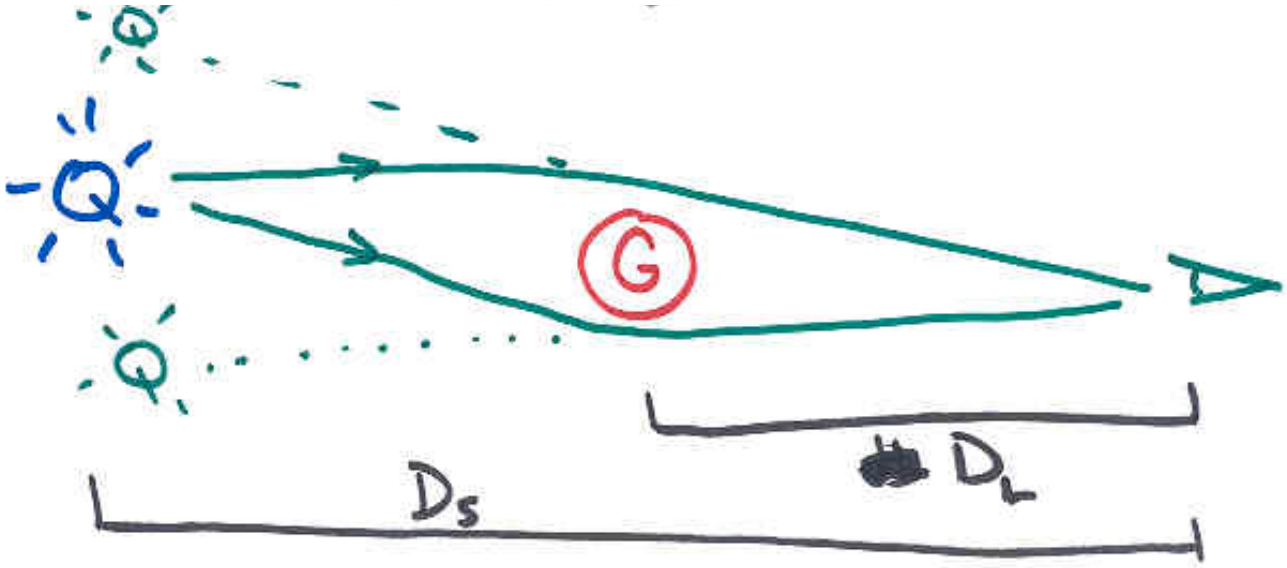

Quasars are variable, and the different images will vary with a lag time between them due to:

- Gravitational potential of the lens
- Path length differences

$\Delta t = f(z_{source}, z_{lens}$, deflection angle, grav potential, cosmology$[H_0,\Omega_M,\Omega_\Lambda])$

Observe….. Model….. Adopt…. Derive

Measuring Time Delays

Not easy:

- Variability is weak (typically ~ few percent)
- Sources are crowded
- Long term monitoring is needed (lots of telescope time)

Example: Q0957+561A/B:
$\Delta t = 417 \pm 3$ days (Kundic+96)

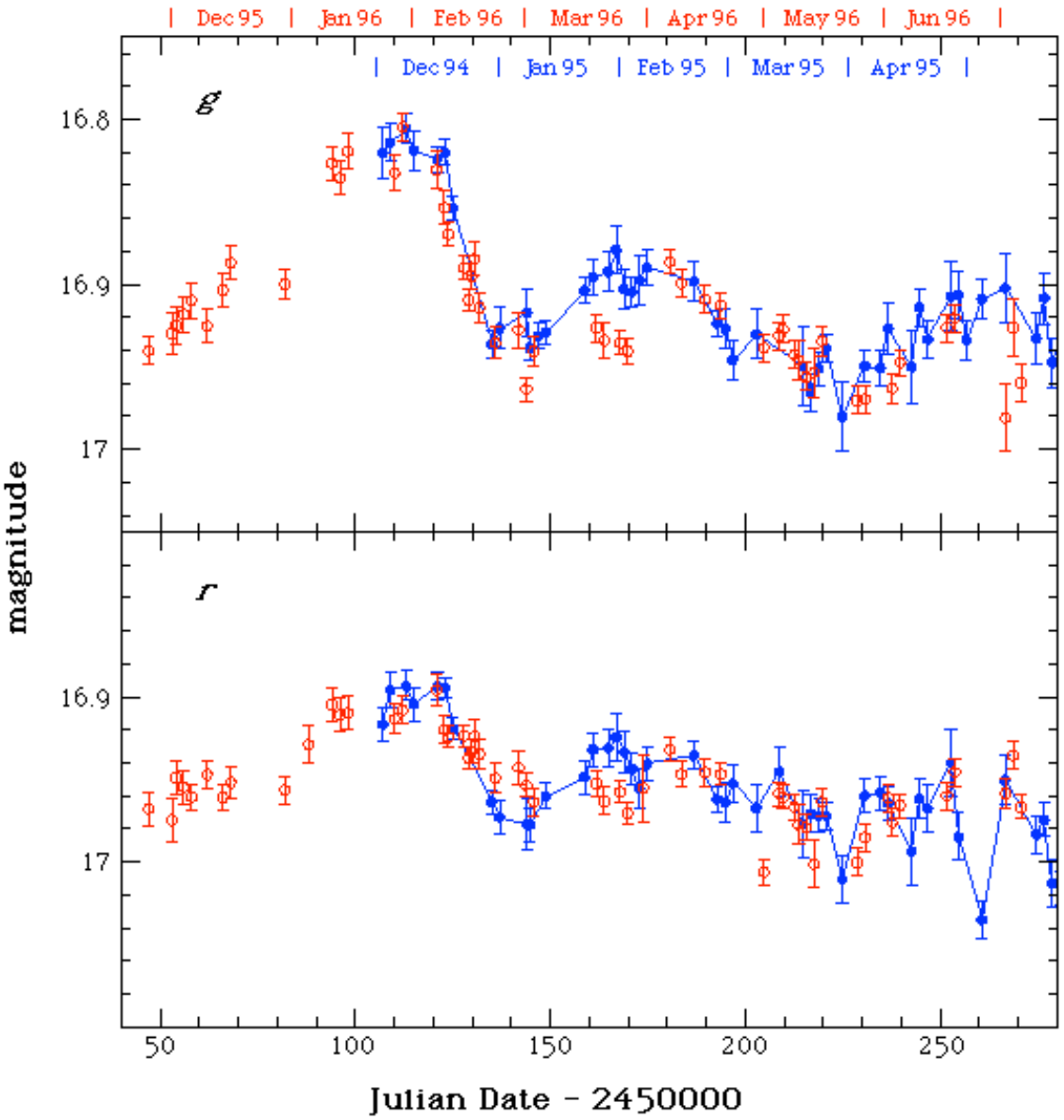

Modeling the lens

Early attempts used point masses. Later models either adopt a dark halo model or else solve for the potential $\Phi(r)$ directly.

Gravitational lenses with multiple images of the source significantly help constrain the model!

Problem: lensing galaxies usually found in galaxy clusters, so there are two potentials to worry about – the galaxy and the cluster. ("mass sheet degeneracy")

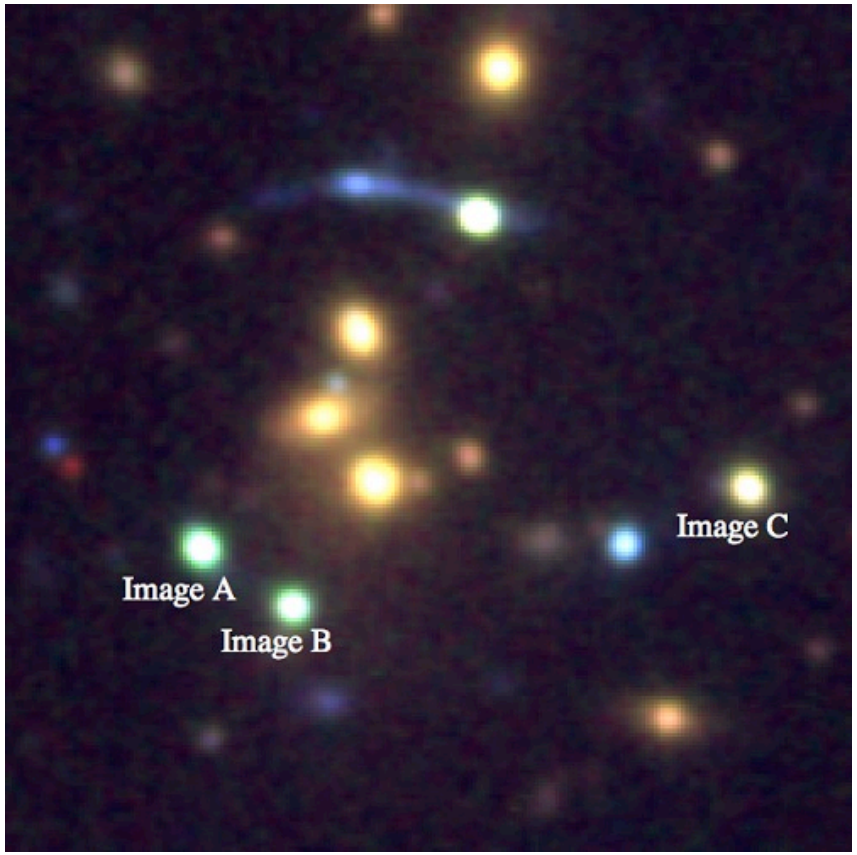

SDSS J2222+2745 (z=2.82)

Recent Results

Lensed Quasar	H0 (km/s/Mpc)	Reference
FBQ 0951+2635	64 +/- 14	Jakobsson+ 05
B0218+357	78 +/- 6	Wucknitz+04
PG 1115+080 and RX J0911+0551	56 +/- 23	Tortora+04
B1608+656	75 +/- 7	Koopmans+03
B1608+656	61-65	Fassnacht+02

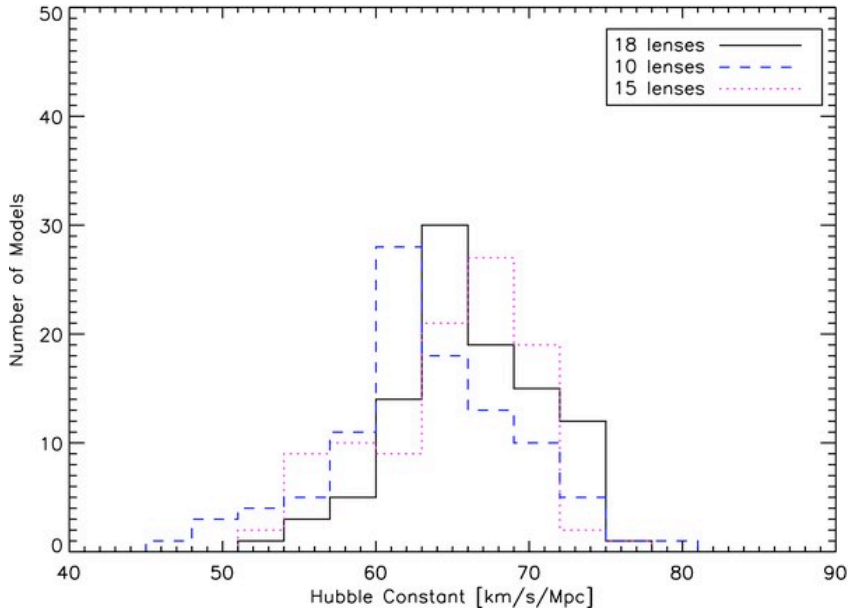

Paraficz & Horth 10
Oguri 07
Saha 06

Recent Results:

B1608+656 (Suyu+10)
RXJ1131-1231 (Suyu+14)
HE0435-1223 (Bonvin+17)

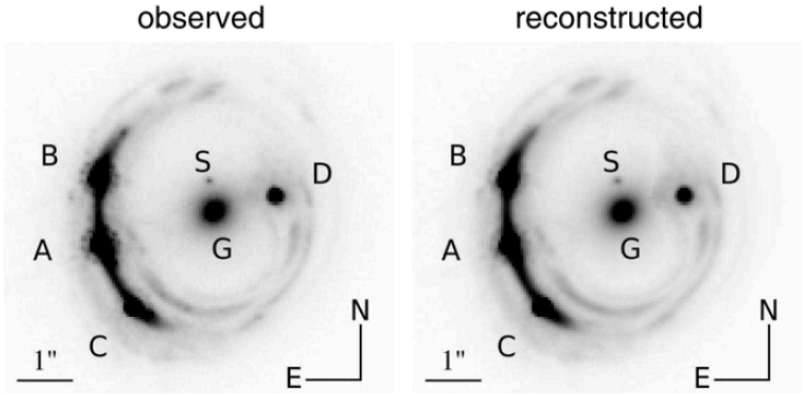

Figure 1. *HST* ACS image of RXJ1131−1231 in *F814W* filter. The background active galactic nucleus is lensed into four images (A, B, C, and D) by the primary lens galaxy G and its satellite S. Left: observed image. Right: reconstructed image based on the most probable composite model in Section 2.2.

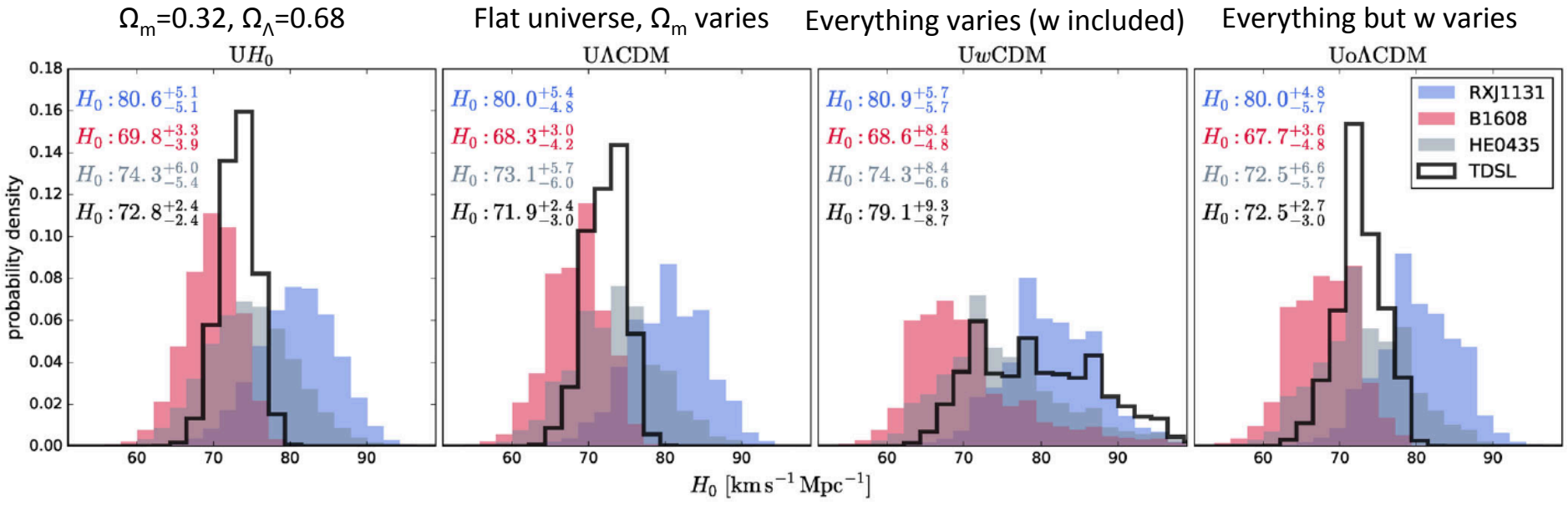

Figure 4. Marginalized posterior probability distributions for H_0 in the UH_0, UΛCDM, UwCDM and UoΛCDM cosmologies using the constraints from the three strong lenses B1608+656, RXJ1131−1231 and HE 0435−1223. The overlaid histograms present the distributions for each individual strong lens (ignoring the other two data sets), and the solid black line corresponds to the distribution resulting from the joint inference from all three data sets (TDSL). The quoted values of H_0 in the top-left corner of each panel are the median, 16th and 84th percentiles.

Supernova lensing

Supernova Refsdal
Found November 2014
(Kelly+15)

Didn't have an accurate time delay, since it was discovered archivally.

But lensing models predicted a new appearance in late 2015…

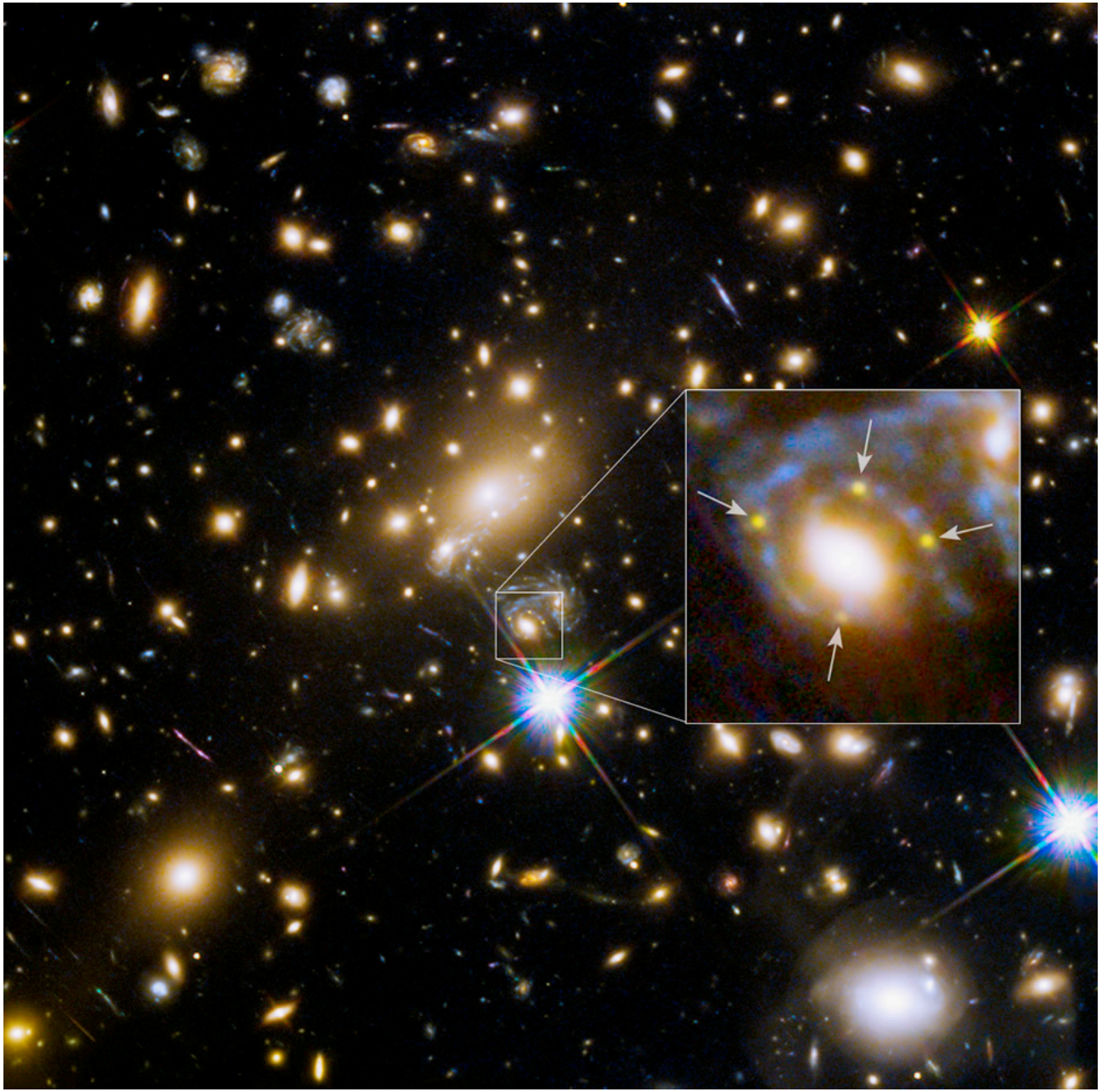

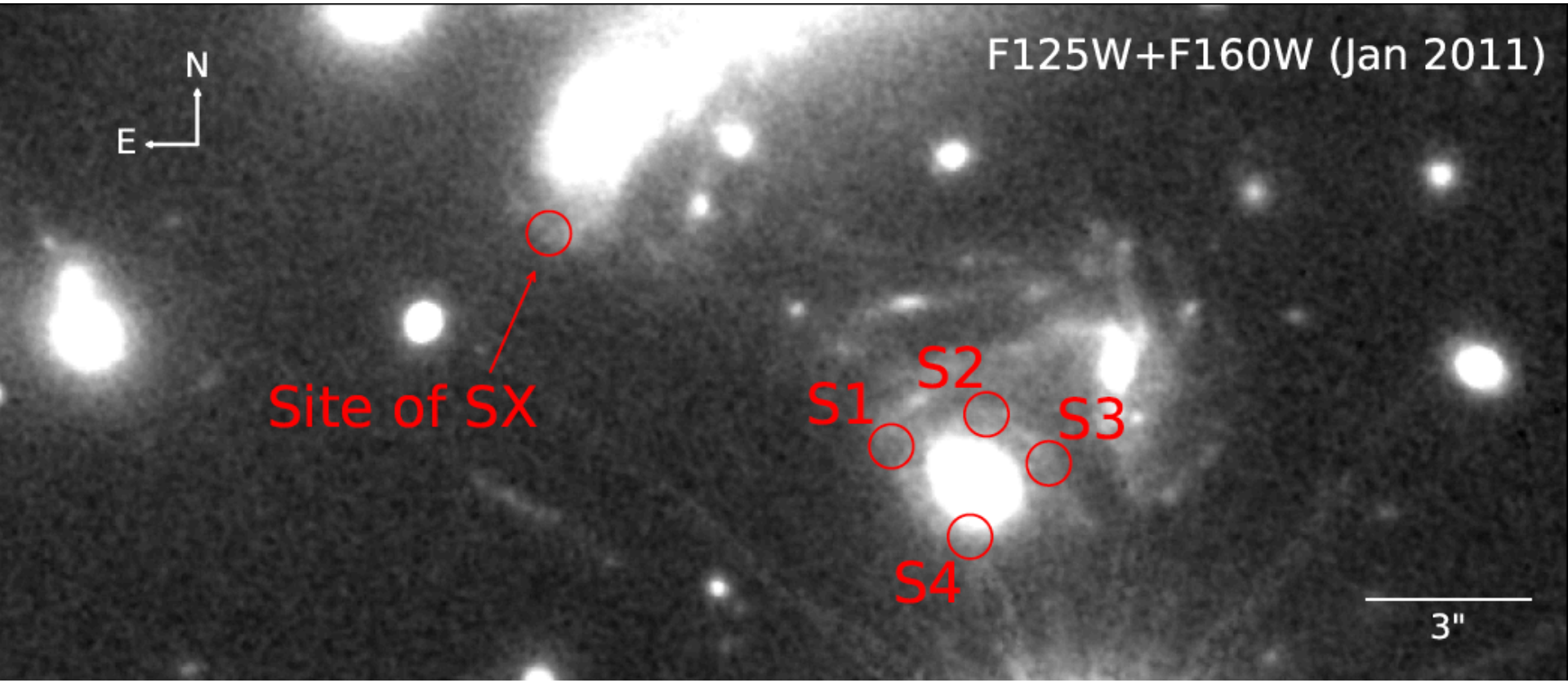
N
E
F125W+F160W (Jan 2011)
Site of SX
S1
S2
S3
S4
3"

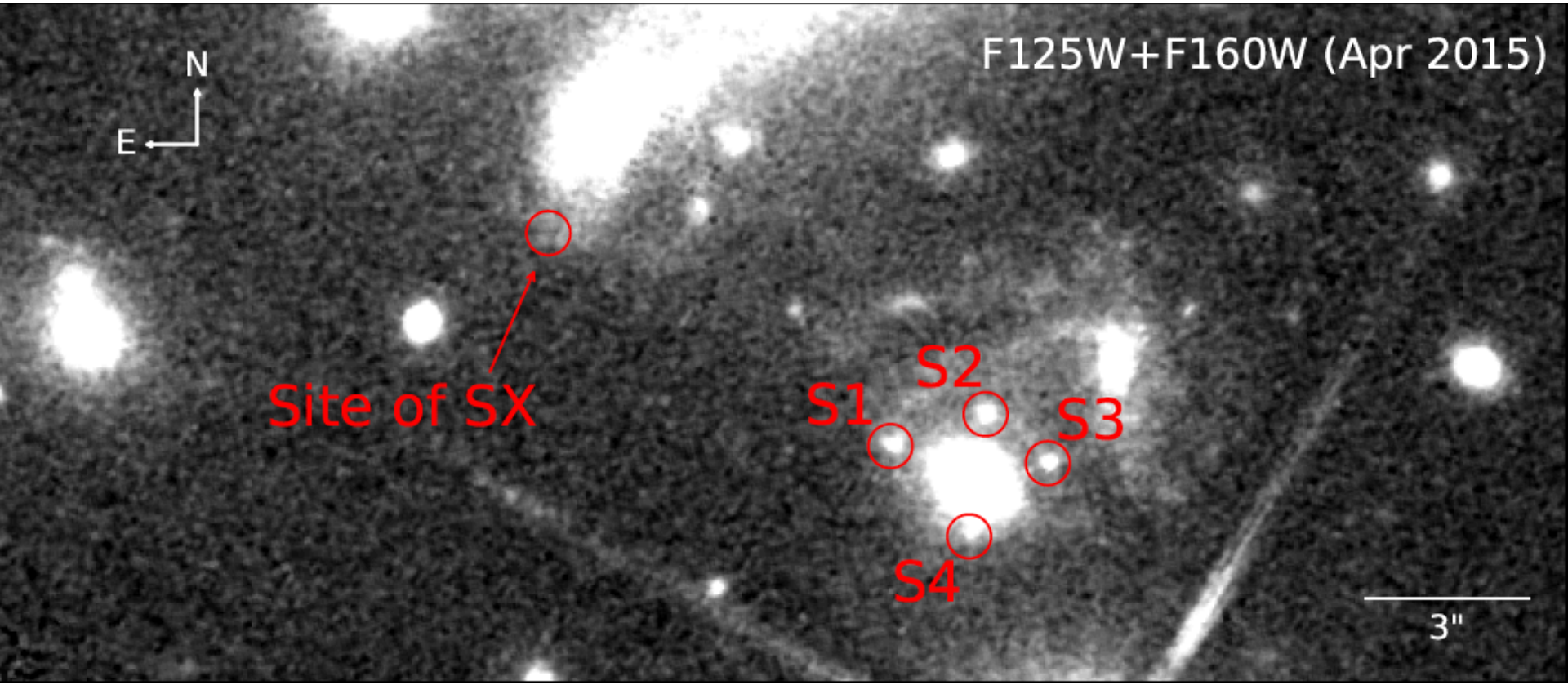
F125W+F160W (Apr 2015)
N
E
Site of SX
S1
S2
S3
S4
3"

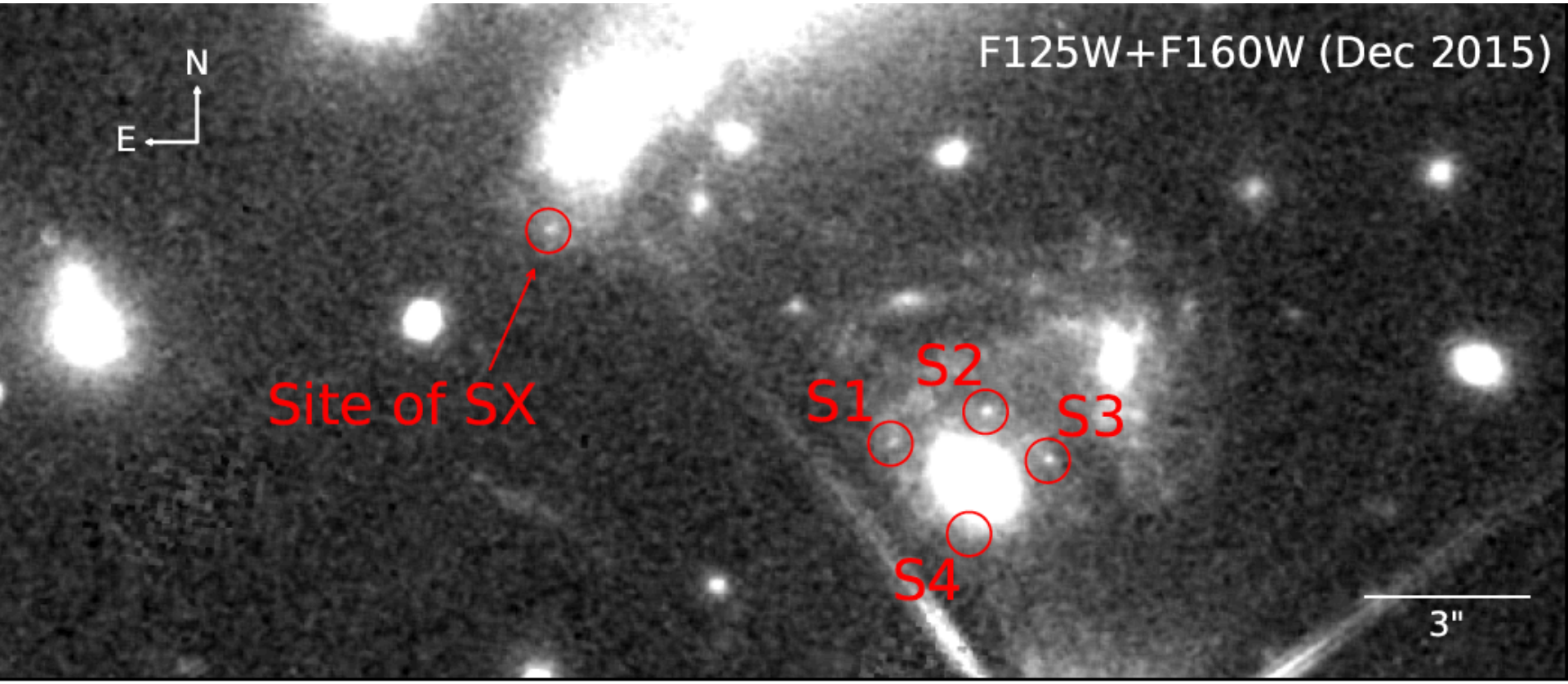
F125W+F160W (Dec 2015)
N
E
Site of SX
S1
S2
S3
S4
3"

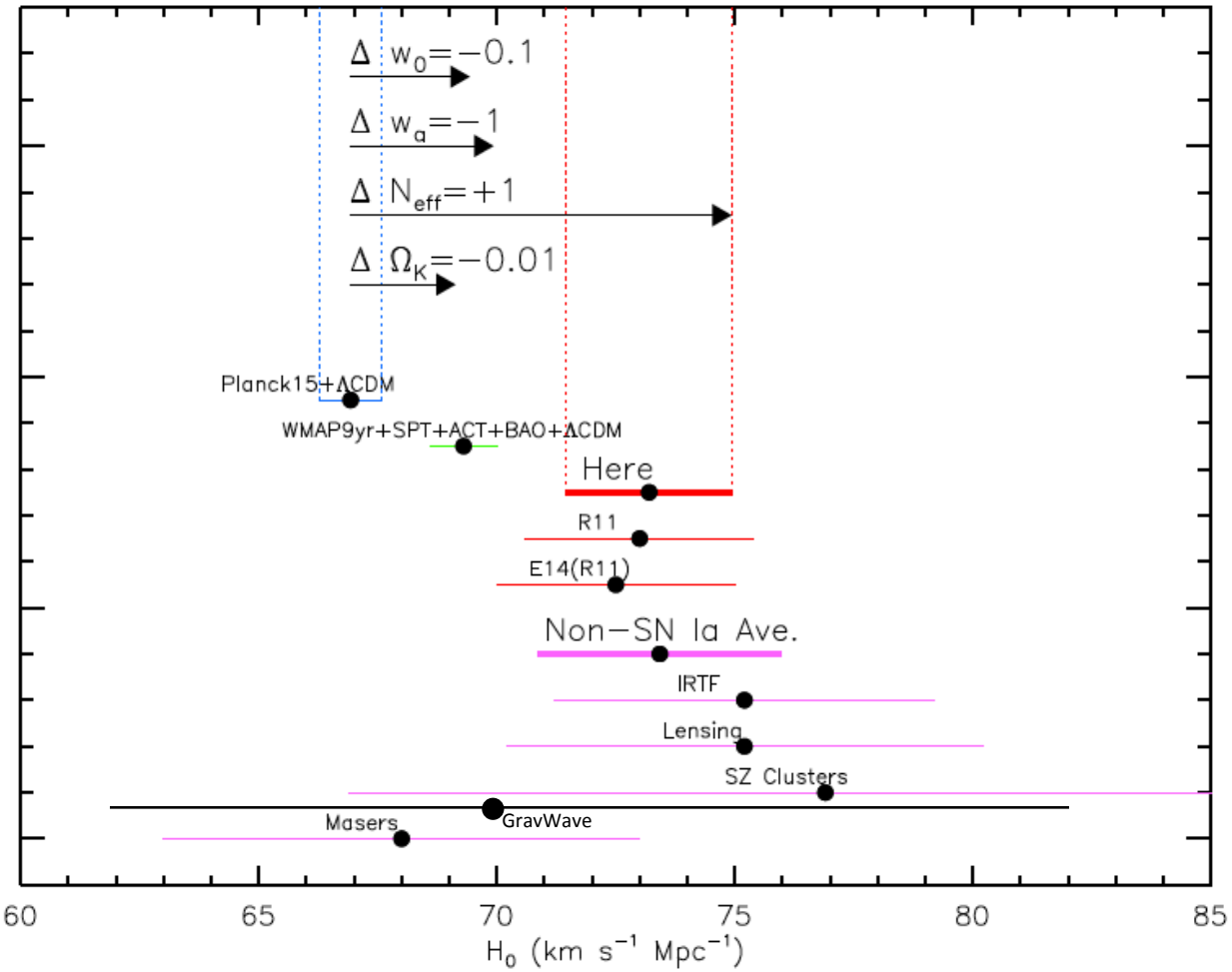

Figure 13. Local measurements of H_0 compared to values predicted by CMB data in conjunction with ΛCDM. We show 4 SN Ia-independent values selected for comparison by Planck Collaboration et al. (2014) and their average, the primary fit from R11, its reanalysis by Efstathiou (2014) and the results presented here. The 3.4σ difference between *Planck*+ΛCDM (Planck Collaboration et al. 2016) and our result motivates the exploration of extensions to ΛCDM.